Magnetotransport in the two-dimensional Lorentz gas

A. Kuzmany* and H. Spohn[†]

Theoretische Physik, Ludwig-Maximilians-Universität, Theresienstrasse 37, D-80333 München, Germany
(Received 3 October 1997)

We consider the two-dimensional Lorentz gas with Poisson-distributed hard-disk scatterers and a constant magnetic field perpendicular to the plane of motion. The velocity autocorrelation is computed numerically over the full range of densities and magnetic fields with particular attention to the percolation threshold between hopping transport and pure edge currents. The corresponding Ohmic and Hall conductances are compared with (i) an exact expression in the percolating regime, (ii) mode-coupling theory, and (iii) a recent generalized kinetic equation valid for low densities and small fields. We argue that the long-time tail as t^{-2} persists for a nonzero magnetic field. [S1063-651X(98)10705-5]

I. INTRODUCTION

Two-dimensional electron films can be manufactured with high perfection in GaAs heterostructures. At low temperatures a mean free path of over 10^4 nm is reached and to a very good approximation the electrons may be considered as noninteracting. To have some interesting physics one nanostructures the probe by lithographic or other techniques. Thereby a strongly repulsive potential is imposed on the electrons with a maximum above the Fermi energy (*quantum antidots*). If the imprinted structure is on a scale larger than the Fermi wavelength, adjustable to be of the order of 50 nm, one hopes to capture the transport properties already in the classical approximation.

So far, the most popular geometry has been a regular array of antidots that corresponds classically to the Sinai billard and should result quantum mechanically in the Hofstadter butterfly. The magnetotransport of this periodic structure has been studied in great detail, both experimentally [1–4] and theoretically [5–8]. In our paper we investigate randomly placed antidots. To our knowledge, the so far best experimental realization has been achieved by Lütjering [9]. We compare our results with his measurements in Sec. V.

In kinetic theory randomly distributed scatterers are known as the Lorentz gas, which has proved to be an important testing ground. In particular, one can understand precisely the assumptions for the validity of the (linear) Boltzmann equation [10] and check on the accuracy of the low-density expansion and its nonanalytic character [11–16]. Also the long-time tails in the velocity autocorrelation function are seen most convincingly in the Lorentz gas [17]. In distinction from the work mentioned, we investigate here the dynamics in the presence of a magnetic field perpendicular to the plane of motion.

The model has a strong geometric quality. One places randomly disks (the scatterers) of radius a in the plane at density n_s. The disks may overlap. In the region outside the disks we have independent point particles with density n_e. They have mass m^*, charge e, and move in a uniform ex-

ternal magnetic field B_{ex}. Thus a single particle travels along a circle and is elastically reflected upon collision with a scatterer. We denote the velocity of the particle at time t by $\mathbf{u}(t)$. Clearly, $|\mathbf{u}(t)|$ is conserved and we set it equal to the Fermi velocity v_F, since at low temperatures contributions to the transport only come from the Fermi surface. The radius of gyration is then $R_e = v_F m^*/eB_{ex}$.

We are interested in the magnetotransport that relates the steady-state current $\mathbf{j}$ to an in-plane uniform electric field $\mathbf{E}$ by

$$\mathbf{j} = \sigma \mathbf{E} \tag{1.1}$$

for small $\mathbf{E}$ and want to understand how σ depends on B_{ex} and n_s. σ_{11} and σ_{22} are the Ohmic conductivities. In our case $\sigma_{11} = \sigma_{22}$ by isotropy. $\sigma_{12} = -\sigma_{21}$ is the Hall conductivity. The magnetotransport will be studied in linear response. This means that the dynamics is the one just explained (*zero electric field*) and the transport coefficients are given in terms of the time-integrated velocity autocorrelation functions. Physically, one has to average over all of the phase space. For a large sample, this is equivalent to fixing the initial position and averaging over the scatterer distribution. It is this prescription that we will use both theoretically and in the numerics. Before spelling out the details we introduce dimensionless quantities.

Space is measured in units of the disk radius a and velocity in units of the Fermi velocity v_F. The scatterers have then radius 1 and their dimensionless density is $\rho = n_s a^2$. The dimensionless radius of gyration is $R = R_e/a$ and the corresponding magnetic field is $B = 1/R = eaB_{ex}/v_F m^*$. Let $\mathbf{v}(t) = \mathbf{u}(t)/v_F$ be the velocity of the particle at time t starting at the origin. Clearly $|\mathbf{v}(t)| = 1$. $\mathbf{v}(t)$ depends on $\mathbf{v}(0)$ and the particular configuration of the scatterers.

We define the dimensionless velocity autocorrelation function by

$$C_{ij}(t) = \langle v_i(0)v_j(t) \rangle, \quad i,j = 1,2. \tag{1.2}$$

Here $\langle \ \rangle$ is a double average. First there is an average over scatterers. The centers of the disks are distributed according to a Poisson process with uniform density ρ conditioned on the set $\{\mathbf{x} \,|\, |\mathbf{x}| \leq 1\}$ being free of centers. Second we average

over the initial velocity $\mathbf{v}(0)=(\cos\varphi,\sin\varphi)$ uniformly in φ. (By rotational invariance this second average could be omitted, but it is of advantage numerically.) The conductivity tensor is then

$$\sigma_{ij}=\frac{n_e e^2}{m^*}\,D_{ij}, \quad D_{ij}=\int_0^\infty dt\,\langle v_i(0)v_j(t)\rangle. \quad (1.3)$$

D depends on ρ and B. Also of interest is the frequency-dependent conductivity defined by

$$\sigma_{ij}(\omega)=\frac{n_e e^2}{m^*}\,D_{ij}(\omega), \quad D_{ij}(\omega)=\int_0^\infty dt\,e^{i\omega t}\langle v_i(0)v_j(t)\rangle. \quad (1.4)$$

We note that $\langle v_i(0)v_j(t)\rangle=\langle v_j(0)v_i(-t)\rangle$ by stationarity and $\langle v_1(0)v_2(t)\rangle=-\langle v_1(0)v_2(-t)\rangle=-\langle v_2(0)v_1(t)\rangle$ by time reversal. Therefore, $D_{12}=-D_{21}$ and $D_{ii}=(1/4)\int_{-\infty}^\infty dt\,\langle\mathbf{v}(0)\cdot\mathbf{v}(t)\rangle$.

As shown in Eq. (1.3), the conductivity is ill defined. There is always a nonzero probability that the particle will not be scattered at all. If so, $\langle v_1(0)v_1(t)\rangle=(1/2)\cos(Bt)$ and $\langle v_1(0)v_2(t)\rangle=(1/2)\sin(Bt)$ and the time integral in Eq. (1.3) needs a reinterpretation. Physically, there will always be a weak elastic scattering by impurities, i.e., once in a while the velocity direction is randomized. In approximation, the velocity autocorrelation function is then modified to

$$e^{-t/\tau}\langle v_i(0)v_j(t)\rangle \quad (1.5)$$

and the proper definition reads

$$D_{ij}(\omega)=\lim_{\tau\to\infty}\int_0^\infty dt\,e^{-t/\tau}e^{i\omega t}\langle v_i(0)v_j(t)\rangle. \quad (1.6)$$

At zero density, no scattering, Eq. (1.6) results in

$$D_{11}(\omega)=-i\,\frac{\omega}{2}\,\frac{1}{B^2-\omega^2}, \quad D_{12}(\omega)=\frac{B}{2}\,\frac{1}{B^2-\omega^2}, \quad (1.7)$$

as is well known from the Drude theory of the Hall effect. In particular, at $\omega=0$ both the Ohmic conductivity and the Ohmic resistance vanish.

It is instructive to return for a moment to the case of an in-plane electric field $\mathbf{E}$. One finds that for freely moving particles the average current approaches

$$\mathbf{j}=\frac{1}{2B}\,(-E_2,E_1) \quad (1.8)$$

as $t\to\infty$, in accordance with Eq. (1.7) at $\omega=0$. In fact, one would expect that scattering cannot make things worse. Thus, for the Lorentz gas there should be a well-defined steady-state current $\mathbf{j}$ for $B\neq0$. We did not find a general argument to establish its existence. The situation at $B=0$ is very different. Then the particle is accelerated along the direction of $\mathbf{E}$. Since only the velocity direction is randomized by collisions, the energy input from the electric field cannot be dissipated and no meaningful steady-state current is reached as $t\to\infty$. However, for small $\mathbf{E}$ the time-dependent

current settles at a plateau over a time span the longer the smaller $\mathbf{E}$, whose value equals $\sigma\mathbf{E}$ with σ of Eq. (1.3).

A brief outline of the paper is as follows. In Sec. II we discuss the dependence of D on ρ,B with particular attention to the two percolation thresholds. We also compare our numerics with the mode-coupling theory of Götze and Leutheußer [18], which seems to be the only theoretical prediction at intermediate densities. Recently, Bobylev *et al.* [19] derived a generalized transport equation for low scatterer densities and small fields. In the appropriate domain of validity their predictions are in fact very accurate (Sec. III) and clearly improve on the phenomenological Boltzmann equation with magnetic field. One of the famous results on the Lorentz gas at $B=0$ is the slow decay of the velocity autocorrelation function as $-t^{-2}$ for large t in two dimensions [20]. For densities $\rho<0.25$ such a power law has been well established numerically [17]. At larger densities there is a preasymptotic decay approximately as $-t^{-1.4}$ and, with reasonable numerical effort, the true asymptotics cannot be seen anymore. In Sec. IV we argue that also for $B\neq0$ the velocity autocorrelation decays as t^{-2} for large t. We conclude in Sec. V with a comparison with the experiments of Lütjering and with some comments.

II. STATIC CONDUCTIVITY

To discuss D in its dependence on ρ,B at zero frequency it is useful to consider first the limiting cases. As explained $D_{11}(0,B)=0$ and $D_{12}(0,B)=1/2B$ at $\rho=0$. On the other hand, for $B=0$ we have $D_{12}(\rho,0)=0$. $D_{11}(\rho,0)$ has been studied numerically [16,17]. For $\rho\to0$ one obtains the Boltzmann value $D_{11}(\rho)=3/16\rho$. Thus, close to $(\rho,B)=0$, D is somewhat singular and roughly of the form $(\rho^2+B^2)^{-1/2}$. Its precise functional dependence will be discussed in Sec. III.

As the density is increased the disks percolate. This means that for $\rho>\rho_c$, $\rho_c\cong0.36$, with probability one the origin is contained in a finite domain bounded by scatterers. For $\rho<\rho_c$ the origin is connected to infinity by a path not intersecting the scatterers. Close to ρ_c numerically one finds $D_{11}(\rho,0)\cong|\rho-\rho_c|^{1.5}$, $\rho\lesssim\rho_c$, with no theoretical explanation yet.

In fact, the Lorentz gas has a second percolation threshold. Let us fix $\rho<\rho_c$ and increase B. Above some critical value B_c, the trajectory will either be a circle or skip along a, possibly large, cluster of a finite number of disks. The bulk current for $B<B_c$ is reduced to a pure edge current. Since the particle cannot leave a cluster, the mean-square displacement is bounded, which implies that $D_{11}(\rho,B)=0$ for $B>B_c$ by the Einstein relation $2D_{11}=\lim_{t\to\infty}\langle\mathbf{r}^2(t)\rangle/2t$. A hopping of the particle from cluster to cluster is possible only if disks with radius $1+R$ percolate, which means, in our units, that $\rho(1+R)^2\geqslant\rho_c$, i.e.,

$$B_c=\frac{1}{\sqrt{\rho_c/\rho}-1}. \quad (2.1)$$

Strictly speaking, the B_c of Eq. (2.1) is only an upper bound on the true B_c. One could imagine that already for a slightly smaller B hopping is suppressed. Numerically, we see a
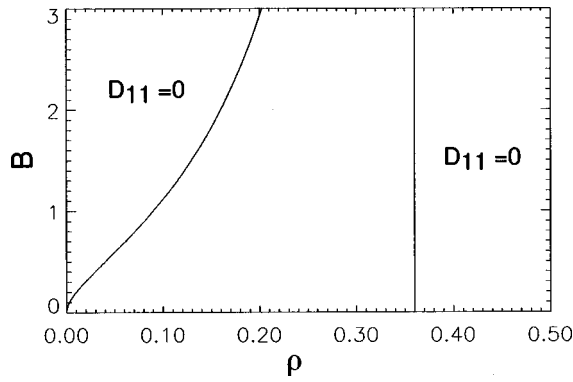
FIG. 1. Percolation thresholds for the Lorentz gas.

smooth variation through B_c and such a fine point cannot be decided. In Fig. 1 we plot the two domains in which the Ohmic conductivity vanishes.

The theoretical discussion of D_{12} above criticality requires more effort. We defer it to the Appendix, where we show that

$$D_{12}=0, \quad \rho>\rho_c \tag{2.2}$$

and

$$D_{12}=\frac{1}{2B}e^{\pi\rho}, \quad \rho<\rho_c, \quad B>B_c. \tag{2.3}$$

For $\rho>\rho_c$ the edge currents move oppositely, whereas for $\rho<\rho_c$ and $B>B_c$ the edge currents move along the current of a particle without collisions. While this gives the right tendency it does not explain the exact cancellations in Eqs. (2.2) and (2.3). They can be understood qualitatively by add-
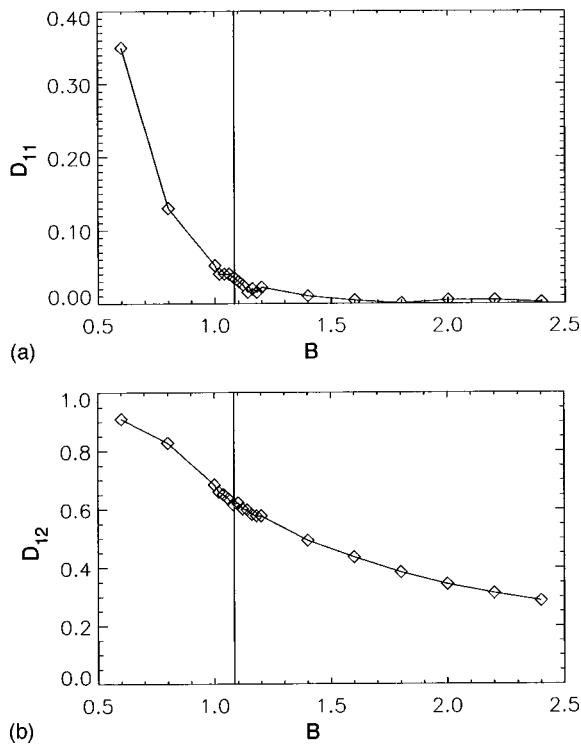
FIG. 2. (a) Ohmic conductivity D_{11} and (b) Hall conductivity D_{12} as functions of B for $\rho=0.1$ in dimensionless units.
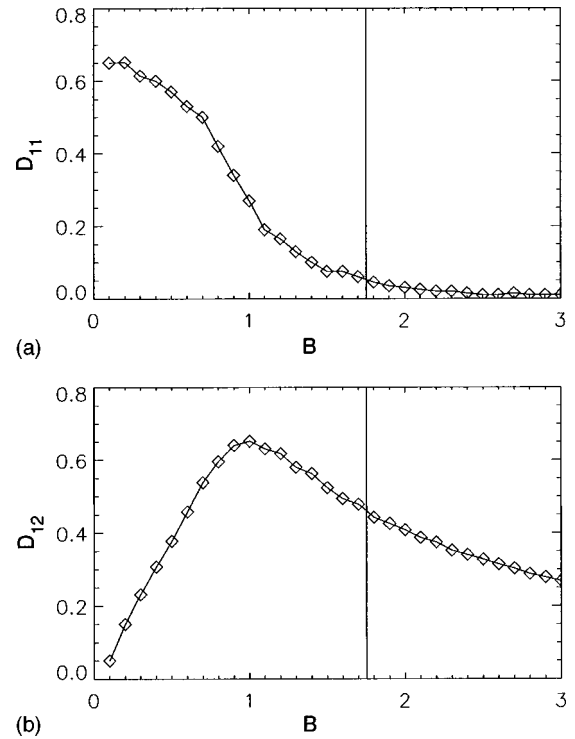
FIG. 3. (a) Ohmic conductivity D_{11} and (b) Hall conductivity D_{12} as functions of B for $\rho=0.15$ in dimensionless units.

ing in a small external electric field $\mathbf{E}=(E,0)$. For $\rho>\rho_c$ the particle moves in a domain bounded by scatterers and therefore cannot maintain a Hall current. On the other hand, for $\rho<\rho_c$ and $B>B_c$, the particle circles several times around a cluster of scatterers until it escapes. It then moves with speed E/B perpendicular to $\mathbf{E}$ until it hits the next cluster. Thus the Hall current is proportional to $1/B$. To us it came as a surprise that beyond percolation D_{12} can still be presented in closed form.

To have a more complete picture of D we simulate the Lorentz gas numerically. For given B and scatterer configuration we compute $v_j(t)$ up to 60 collision times. The system size is chosen so large that $\mathbf{x}(t)=\int_0^t ds\,\mathbf{v}(s)$ never hits the boundary. To speed up the simulation we use a hierarchical search for the next point of collision. For each scatterer configuration we average over 100 randomly chosen initial velocity directions. For $C_{ij}(t)$ to be sufficiently smooth typically one has to average then over 10^6 sample paths. To determine the conductivity we integrate the velocity autocorrelation once to give $\langle v_i(0)x_j(t)\rangle$ since $x_j(0)=0$. Furthermore, it is convenient to separate off the contribution of circle orbits. According to the Poisson distribution, their probability is $\exp[-\pi\rho\kappa(R)]$, with $\kappa(R)=R(R+2)$ for $R<1$ and $\kappa(R)=4R-1$ for $R\geq 1$. Then

$$D_{ij}=\lim_{t\to\infty}\langle v_i(0)x_j(t)\rangle_1+(1-\delta_{ij})\frac{R}{2}e^{-\pi\rho\kappa(R)}, \tag{2.4}$$

where $\langle\ \rangle_1$ is the average over only those trajectories that have at least one collision. The normalization is $\langle 1\rangle_1=1 -\exp[-\pi\rho\kappa(R)]$. In most of the parameter space $\langle v_i(0)x_j(t)\rangle$ has not yet reached its asymptotic value, which reflects the slow decay of the velocity autocorrelation func-
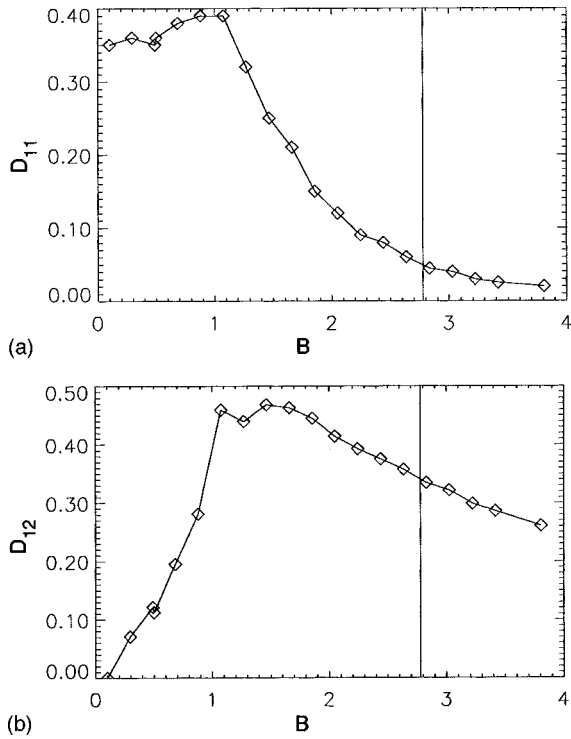
FIG. 4. (a) Ohmic conductivity D_{11} and (b) Hall conductivity D_{12} as functions of B for $\rho = 0.2$ in dimensionless units.

tions. We essentially extrapolate ''by hand'' to $t \to \infty$, which results in a slight overestimate whenever there is an independent check.

In Figs. 2–5 we display our results at densities $\rho = 0.1, 0.15, 0.2$, and 0.3. The percolation threshold is indicated by a vertical line. Note that for $\rho = 0.1$ the B scale
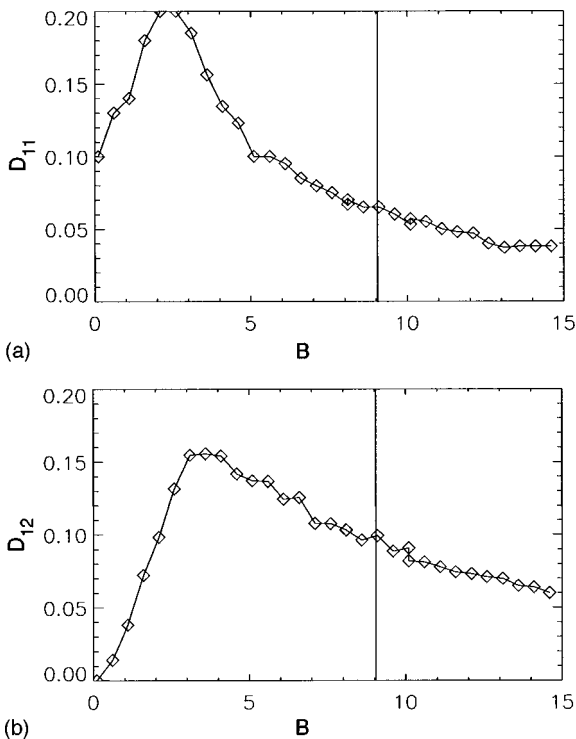
FIG. 5. (a) Ohmic conductivity D_{11} and (b) Hall conductivity D_{12} as functions of B for $\rho = 0.3$ in dimensionless units.
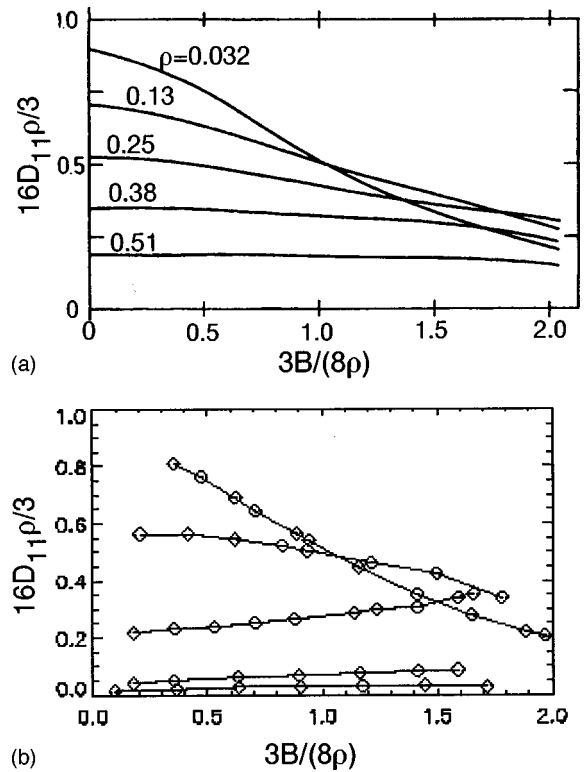
FIG. 6. (a) Ohmic conductivity D_{11} according to the mode-coupling theory of [18] for various densities. (b) Simulation data of the Ohmic conductivity D_{11} for the same densities and in the same units as in (a).

starts at $B = 0.5$. Our data show a fairly smooth interpolation of the asymptotics at $B = 0$ and $B = \infty$. The most surprising feature is an initial increase of the Ohmic conductivity with B at intermediate densities. Apparently, the curved trajectory can bend itself more easily through the dense ''labyrinth'' of scatterers. The Hall conductivity rises steeply to its maximum and then levels off. The maximum is shifted to smaller B as the density decreases. For $B > B_c$ the agreement with Eq. (2.3) is excellent and within numerical error bars, except at the highest density of 0.3, where the numerical values are 25% below the theoretical prediction.

To our knowledge, the only attempt to derive the magnetoconductivity at intermediate densities is the mode-coupling theory of Götze and Leutheuβer [18]. In Fig. 6 we compare their prediction with our simulation data; note the particular choice of units. For the lowest density $\rho = 0.032$, we find good agreement. Essentially the same behavior is obtained from the generalized Boltzmann equation, to be discussed in the following section. However, the kinetic theory fails at density $\rho = 0.13$, whereas mode coupling is still a reasonable approximation. The next higher density $\rho = 0.25$ can no longer be accounted for.

III. LOW DENSITY, SMALL FIELDS

For $B = 0$ the linear Boltzmann equation is exact at low density. More precisely, for $\rho \to 0$ collisions of the particle with the same scatterer become unlikely and the density of particles in phase space on the scale of the mean free path is governed by the Boltzmann equation. In particular, this

yields $D_{11}(\rho,0)=3/16\rho$ as $\rho\to0$. With an external magnetic field B one generalizes in the obvious way to

$$\partial_t f(\mathbf{x},\varphi,t)=(-\cos\varphi\partial_1-\sin\varphi\partial_2-B\partial_\varphi)f(\mathbf{x},\varphi,t)$$

$$+2\rho\int_{-\pi}^{\pi}d\varphi'\,\frac{1}{4}\,\sin\left|\frac{\varphi'}{2}\right|[f(\mathbf{x},\varphi-\varphi',t)$$

$$-f(\mathbf{x},\varphi,t)].\qquad(3.1)$$

Here f is the distribution function at $\mathbf{x}$, $\mathbf{v}=(\cos\varphi,\sin\varphi)$, and t. On the basis of Eq. (3.1) one obtains

$$D_{11}^0=\frac{1}{2}\,\frac{8\rho/3}{(8\rho/3)^2+B^2},\quad D_{12}^0=\frac{1}{2}\,\frac{B}{(8\rho/3)^2+B^2},\quad(3.2)$$

which we rewrite in a scaling form as

$$D_{11}^0=\frac{1}{\sqrt{\rho^2+B^2}}\,g_{11}^0(\rho/B),$$

$$D_{12}^0=\frac{1}{\sqrt{\rho^2+B^2}}\,g_{12}^0(\rho/B),$$

$$g_{11}^0(y)=\frac{1}{2}\sqrt{1+y^2}\,\frac{8y/3}{(8y/3)^2+1},$$

$$g_{12}^0(y)=\frac{1}{2}\sqrt{1+y^2}\,\frac{1}{(8y/3)^2+1}.\qquad(3.3)$$

For a rigorous derivation the radius of gyration must be of the order of the mean free path. Thus B must vanish linearly with ρ. As observed by Bobylev *et al.* [19], even in the limit $\rho\to0$ some recollisions survive. This is most easily seen for circle orbits with no collisions at all. According to the Boltzmann equation (3.1), even after several turns the particle still has some probability to be scattered. However, for the mechanical Lorentz gas after one completed revolution the annulus is surely free of disks and no scattering events can occur. In [19] the circling orbits and the recollisions are properly taken into account for $\rho\to0$ and a generalized kinetic equation with memory term is derived. On this basis the velocity autocorrelations are computed. The conductivity is still of the scaling form (3.3),

$$D_{11}^*=\frac{1}{\sqrt{\rho^2+B^2}}\,g_{11}^*(\rho/B),$$

$$D_{12}^*=\frac{1}{\sqrt{\rho^2+B^2}}\,g_{12}^*(\rho/B),\qquad(3.4)$$

which is just a consequence of $B/\rho=$const as $\rho\to0$. However, the scaling functions are now modified to

$$g_{11}^*(y)=\frac{1}{2}\sqrt{1+y^2}\frac{1}{[2y\,\gamma(x)]^2+1}(1-x^2)2y\,\gamma(x),$$
$$(3.5)$$

(a)

(b)
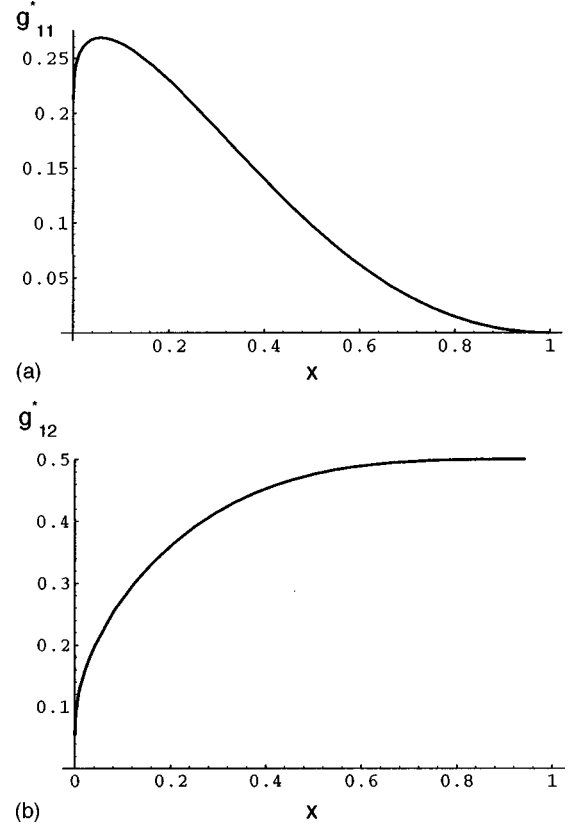
FIG. 7. Scaling functions (a) g_{11}^* and (b) g_{12}^* as functions of $x=e^{-2\pi\rho/B}$.

$$g_{12}^*(y)=\frac{1}{2}\sqrt{1+y^2}\frac{1}{[2y\,\gamma(x)]^2+1}\{1+x^2[2y\,\gamma(x)]^2\},$$
$$(3.6)$$

$$x=e^{-2\pi y},\qquad(3.7)$$

$$\gamma(x)=1-\frac{1-x^2}{2x^2}\left(\frac{1-x^2}{2x}\ln\frac{1+x}{1-x}-1\right).\qquad(3.8)$$

In Fig. 7 we plot g_{11}^*,g_{12}^*. Note that in terms of the polar angle in the ρ-B plane the scale is highly compressed at the left. In Fig. 8 we plot the correction to the Boltzmann value (3.3).

Of course, D^* reproduces the correct limiting behavior for $\rho\to0$ and $B\to0$. According to Eq. (2.1), the percolation boundary behaves as $B_c\cong1.66\sqrt{\rho}$ for small ρ. Since for the validity of Eq. (3.4) B is scaled proportionally to ρ, D^* cannot "see" this threshold.

In Figs. 9 and 10 we compare our numerical results with D^*. We also include D^0. As expected, D^* is a considerable improvement. Note that the agreement is not uniform in $\sqrt{B^2+\rho^2}$. This reflects that at $B=0$ the Boltzmann equation has a restricted range of validity, e.g., $D_{11}(\rho,0)/D_{11}^0(\rho)=0.65$ at $\rho=0.1$.

IV. VELOCITY AUTOCORRELATIONS

On the level of the linear Boltzmann equation (3.1) one obtains an exponential decay for the velocity autocorrelations. Explicitly,
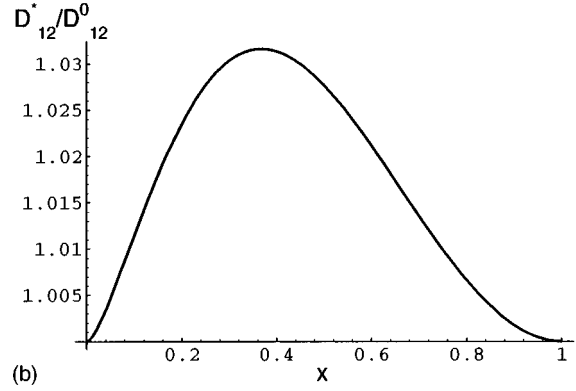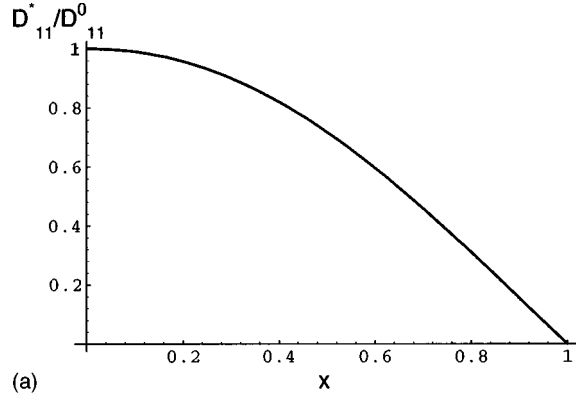
FIG. 8. Ratios (a) D^*_{11}/D^0_{11} and (b) D^*_{12}/D^0_{12} as functions of $x = e^{-2\pi\rho/B}$.
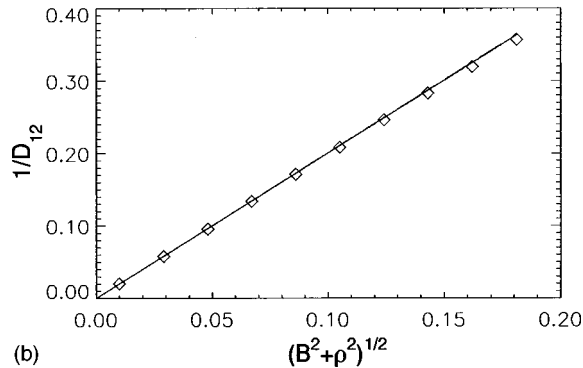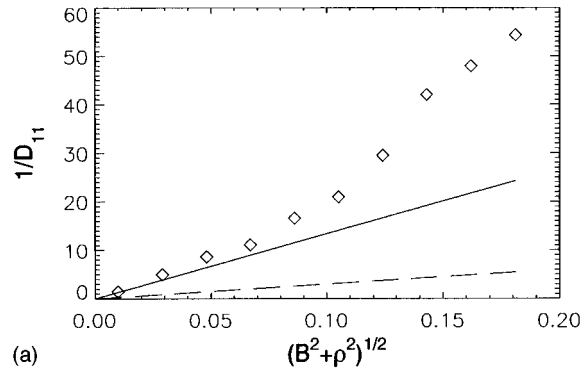
FIG. 9. (a) Inverse Ohmic conductivity $1/D_{11}$ and (b) inverse Hall conductivity $1/D_{12}$ as functions of $(B^2+\rho^2)^{1/2}$ for the fixed ratio $\rho/B=0.025$. - - - is the Boltzmann theory, —— is the improved Boltzmann theory, and $\diamond$ are the simulation data.
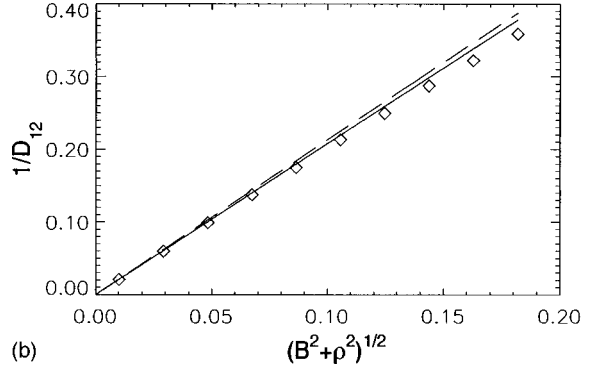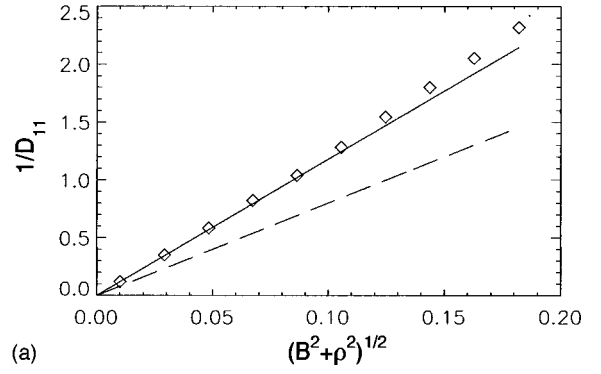
FIG. 10. (a) Inverse Ohmic conductivity $1/D_{11}$ and (b) inverse Hall conductivity $1/D_{12}$ as functions of $(B^2+\rho^2)^{1/2}$ for the fixed ratio $\rho/B=0.1$. - - - is the Boltzmann theory, —— is the improved Boltzmann theory, and $\diamond$ are the simulation data.

$$C^0_{11}(t)=\frac{1}{2}e^{-|t|/\tau_0}\cos(Bt), \quad C^0_{12}(t)=\frac{1}{2}e^{-|t|/\tau_0}\sin(Bt),$$

(4.1)

with $\tau_0=(8\rho/3)^{-1}$. The correct low-density, small-field behavior has a more interesting structure. To state the result it is convenient to introduce the Laplace transforms

$$F(z)=\int_0^\infty dt\ e^{-zt}2[C_{11}(t)+iC_{12}(t)]$$

(4.2)

for $\mathrm{Re}(z)>0$. In the same approximation as that leading to Eq. (3.4) one obtains

$$F(z)=\frac{1-e^{-(z+\nu)T}}{z-i\omega+\nu\int_{-\pi}^{\pi}d\psi\ g(\psi)\dfrac{1-e^{i\psi}}{1-e^{(z+\nu)T+i\psi}}}+\frac{e^{-(z+\nu)T}}{z-i\omega}.$$

(4.3)

We find it convenient to compare the Fourier transforms

$$\hat{C}_{ij}(\omega)=\int_{-\infty}^\infty dt\ e^{-i\omega t}C_{ij}(t)$$

(4.4)

with the simulation data. Since $C_{11}(t)$ is even and $C_{12}(t)$ is odd, we have $\hat{C}_{11}(\omega)=\mathrm{Re}[F(i\omega)+F(-i\omega)]$ and $\hat{C}_{12}(\omega)=i\,\mathrm{Re}[-F(i\omega)+F(-i\omega)]$. The circle orbits yield δ peaks at $\omega=\pm1/R$ with weight $\exp(-4\pi\rho R)$. In Fig. 11 we plot the prediction from Eq. (4.3) and compare it with the numerics. Note that the δ peaks are out of scale. As anticipated, the
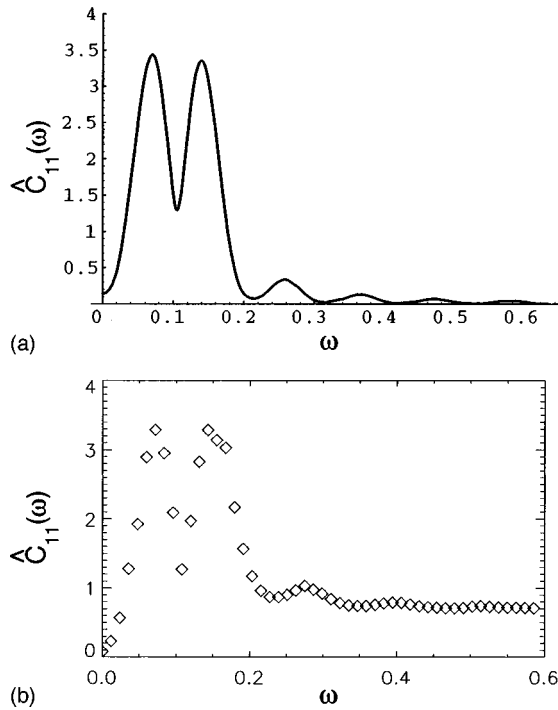
FIG. 11. Real part of $\hat{C}_{11}(\omega)$ with $\rho/B=0.025$ and $(B^2+\rho^2)^{1/2}=0.105$ from (a) the improved Boltzmann theory and (b) the simulation data.

agreement is excellent, in fact, over the whole low-density, small-field regime. We plot $\hat{C}_{12}(\omega)$, which turns out to be negative (Fig. 12). As the ratio ρ/B is increased, the characteristic double peak merges into a single peak, which then shifts to $\omega=0$.
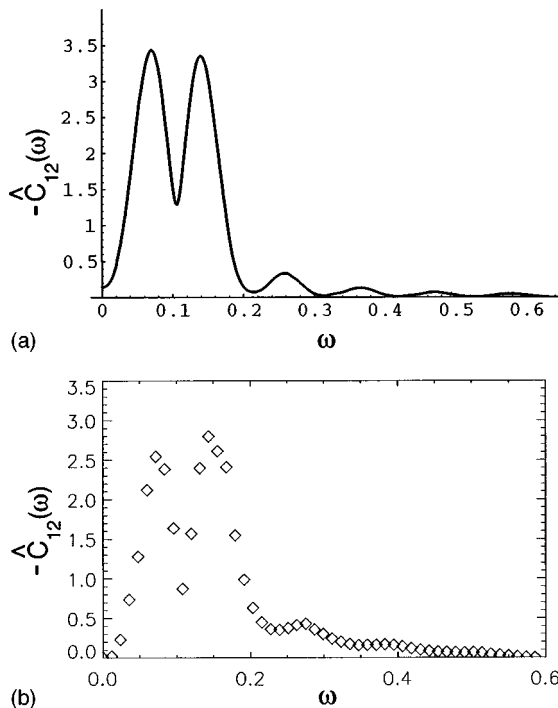
FIG. 12. Negative imaginary part of $\hat{C}_{12}(\omega)$ with $\rho/B=0.025$ and $(B^2+\rho^2)^{1/2}=0.105$ from (a) the improved Boltzmann theory and (b) the simulation data.
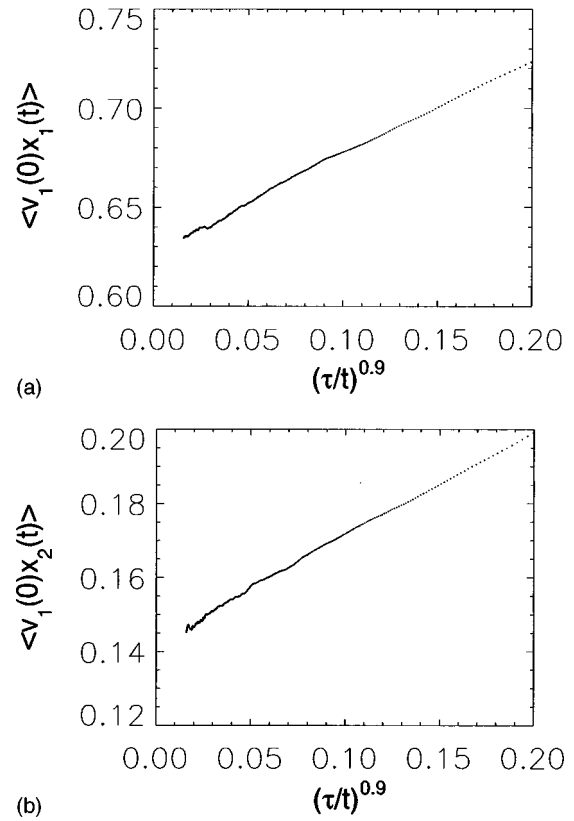
FIG. 13. Integrated velocity autocorrelation functions (a) $\langle v_1(0)x_1(t)\rangle$ and (b) $\langle v_1(0)x_2(t)\rangle$ with $\rho=0.15$ and $B=0.2$ as functions of $(\tau/t)^{0.9}$.

Away from low density and small fields we have no theory to compare with. For $B=0$, $C_{11}(t)$ has the long-time tail of the form $C_{11}(t)=-\alpha t^{-2}$, with $\alpha>0$. We refer to [21] for a detailed discussion. The heuristic explanation is as follows. At long times the main contribution of $C_{11}(t)$ comes from paths returning to the origin at time t. Let $\mathbf{v}(0)=(1,0)$. Then the particle will be more likely to return from the right, which yields a negative correlation in the velocity. For the excursion away from the origin we use a random-walk approximation. If at some intermediate time the particle arrives at the line $x=0$, then it will return to the origin equally likely from right and left and the contribution to $C_{11}(t)$ vanishes. Therefore, the tail can be computed from a return to the origin at time t of a random walker *without* ever hitting the line $x=0$. This probability decays as t^{-2} in two dimensions. Clearly, in our argument we only used that the motion before returning to the origin is diffusive. This remains valid for nonzero B. Thus $C_{11}(t)$ and $C_{12}(t)$ should have a decay as t^{-2} for $t\to\infty$. For $B=0$ the long-time tail is most clearly seen at $\rho=0.15$ [17]. We increase B to 0.2 and average over 3×10^7 sample paths. The effective exponent for both correlations is 1.9 with a negative prefactor (Fig. 13). However, the prefactor of $C_{11}(t)$ becomes positive in the range $B=0.5-0.8$ and of $C_{12}(t)$ in the range $B=0.6-3$. Thus, when the particle returns to the origin it picks up more complicated velocity correlations than in the case $B=0$. As one example of such a sign reversal in the 1,2 correlation we display the data for $\rho=0.2$ and $B=2.3$ (Fig. 14). The effective exponents are approximately 1.4.
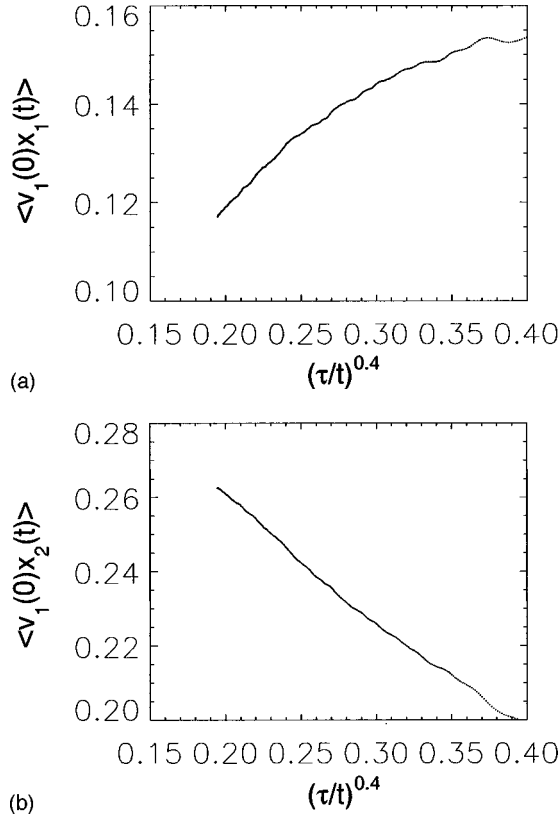
FIG. 14. Integrated velocity autocorrelation functions (a) $\langle v_1(0)x_1(t)\rangle$ and (b) $\langle v_1(0)x_2(t)\rangle$ with $\rho=0.2$ and $B=2.2$ as functions of $(\tau/t)^{0.4}$.

V. DISCUSSION

We studied transport in the two-dimensional Lorentz gas with a constant magnetic field perpendicular to the plane of motion. The theory of Bobylev *et al.* is in fair agreement with our simulation data for both the transport coefficients and the velocity autocorrelations. Away from low density and small magnetic fields there is little theory to compare with. The qualitative properties of the magnetotransport can be guessed from the well-understood limiting cases $B\rightarrow0$ and $B\rightarrow\infty$. The most unexpected feature is an increase in the Ohmic conductivity with increasing B at intermediate densities. Such a behavior has also been found experimentally [9].

In these measurements antidots are imprinted at random locations with densities $1/(1000\ \mathrm{nm})^2$, $1/(600\ \mathrm{nm})^2$, $1/(400\ \mathrm{nm})^2$, $1/(300\ \mathrm{nm})^2$, and $1/(240\ \mathrm{nm})^2$, respectively. The electrons ''feel'' a screened potential. For the periodic case this is usually modeled by $V(x_1,x_2)=V_0|\sin(\pi x_1/a)\sin(\pi x_2/a)|^\beta$, with β ranging from 2 to 4. For a random distribution the true potential is more complicated, in particular, when there is strong overlap. Thus we cannot expect quantitative agreement between our hard-disk model potential and the experiment [9]. There the reduced density roughly ranges from 0.01 to 0.25 in our units. The dimensionless magnetic field varies from 0 to 3. Qualitatively, the conductivities D_{11},D_{12} in dependence on B follow our curves. However, the measured D_{12} is smaller by approximately a factor 1/2. At the largest density a distinct increase in D_{11} with B close to $B=0$ is observed. As in our numerical studies, the percolation threshold B_c is hardly seen

in the Hall conductance. The Ohmic conductivity is small for $B>B_c$, but the transition region is fairly broad.

The velocity autocorrelations have a slow decay over the full range of parameters. Presumably it is governed by t^{-2}, which is, however, severely masked by an even slower preasymptotic decay. The definite sign of the prefactor at $B=0$ is not retained.

ACKNOWLEDGMENT

APPENDIX: HALL CONDUCTIVITY BEYOND PERCOLATION

If either $\rho>\rho_c$ or $B>B_c$, then the position $\mathbf{x}(t)$ of the particle remains uniformly bounded in the course of time. We exploit this property in the computation of D_{12}, but first present a general argument valid for any Hamiltonian system.

Let f,g be bounded functions on phase space and let $\langle\ \rangle_0$ be some finite phase-space average that is stationary, i.e., $\langle f(t)\rangle_0=\langle f(0)\rangle_0$ for all t and functions f. Note that no mixing of $\langle\ \rangle_0$ or the like is required. Then

$$\lim_{\tau\rightarrow\infty}\int_0^\infty dt\ e^{-t/\tau}\langle\dot{f}(t)\dot{g}(t)\rangle_0=-\langle f(0)\dot{g}(0)\rangle_0=\langle\dot{f}(0)g(0)\rangle_0.$$
(A1)

The proof uses twice partial integration

$$\int_0^\infty dt\ e^{-t/\tau}\frac{d}{dt}\langle f(t)\dot{g}(0)\rangle_0$$

$$=-\langle f(0)\dot{g}(0)\rangle_0+\tau^{-1}\int_0^\infty dt\ e^{-t/\tau}\langle f(0)\dot{g}(-t)\rangle_0$$

$$=-\langle f(0)\dot{g}(0)\rangle_0+\tau^{-1}\langle f(0)g(0)\rangle_0$$

$$-\tau^{-2}\int_0^\infty dt\ e^{-t/\tau}\langle f(t)g(0)\rangle_0,$$
(A2)

where we used stationarity in the second step. Since f,g are bounded, the limit $\tau\rightarrow\infty$ yields Eq. (A1).

We first apply Eq. (A1) to the case $\rho>\rho_c$. We assume that the particle moves in some domain, say Λ, bounded by scatterers. As a stationary measure $\langle\ \rangle_0$ we choose $\chi_\Lambda(\mathbf{x})\ d^2x\ d\varphi$, with $\chi_\Lambda(\mathbf{x})=1$ if $\mathbf{x}\in\Lambda$ and $\chi_\Lambda(\mathbf{x})=0$ otherwise.

By Eq. (A1)

$$D_{12}^0=\lim_{\tau\rightarrow\infty}\int_0^\infty dt\ e^{-t/\tau}\langle v_2(t)v_1(0)\rangle_0=-\langle x_2\cos\varphi\rangle_0=0.$$
(A3)

To determine D_{12} we have to compute the double average $\langle\ \rangle$ in Eq. (1.2). The particle starts at 0 and we assume that the scatterers bound its motion to some finite domain Λ. We average now over all translates of this configuration such that 0 is still contained in the translate of Λ. Under the Poisson distribution every translate has the same weight. Therefore,

this partial average coincides with $\langle\ \rangle_0$ and $D_{12}^0 = 0$ by Eq. (A3). Since $\rho > \rho_c$, with probability one $\langle\ \rangle$ decomposes into averages of the form $\langle\ \rangle_0$ and we conclude that $D_{12} = 0$.

Second we apply Eq. (A1) to the case $\rho < \rho_c$ and $B > B_c$. Let $\mathbf{y}_j$, $j = 1, \ldots, N$, be the centers of N scatterers. We choose an arbitrary domain Λ such that

$$\Lambda \supset \{\mathbf{x} | |\mathbf{x} - \mathbf{y}_j| \leqslant R + 1, \quad j = 1, \ldots, N\} \qquad (A4)$$

and define

$$\Lambda_e = \{\mathbf{x} | |\mathbf{x} - \mathbf{y}_j| \geqslant 1, \quad j = 1, \ldots, N\},$$

$$\Lambda_i = \{\mathbf{x} | |\mathbf{x} - \mathbf{y}_j| \leqslant 1, \quad j = 1, \ldots, N\}.$$

As the invariant phase-space density $\langle\ \rangle_N$ we choose

$$h(\mathbf{x}, \varphi) = \frac{1}{2\pi} \chi_{\Lambda_e}(\mathbf{x}) \chi_\Lambda(x_1 - R \sin \varphi, x_2 + R \cos \varphi). \qquad (A5)$$

To check the stationarity we note that at a collision $h(\mathbf{x}, \varphi) = 1/2\pi$. In particular, h takes the same value for the incoming and outgoing velocities. Away from collisions and outside the scatterers $\chi_{\Lambda_e} = 1$ and h is of the general form $f(x_1 - R \sin \varphi, x_2 + R \cos \varphi)$, which does not change under the circling motion.

For given $(\mathbf{x}, \varphi)$ the center of gyration is $(x_1 - R \sin \varphi, x_2 + R \cos \varphi)$. Thus, in Eq. (A5) χ_Λ selects the initial conditions for which the center of gyration is in Λ, whereas χ_{Λ_e} makes sure that the initial condition does not overlap with a scatterer.

The normalization of h is easily determined as

$$\frac{1}{2\pi} \int d\varphi \int d^2x\ \chi_{\Lambda_e}(\mathbf{x}) \chi_\Lambda(x_1 - R \sin \varphi, x_2 + R \cos \varphi)$$

$$= \frac{1}{2\pi} \int d\varphi \int d^2x\ \chi_{\Lambda_e} + (x_1 - R \sin \varphi, x_2 + R \cos \varphi)$$

$$\times (\mathbf{x}) \chi_\Lambda(\mathbf{x}) = |\Lambda \backslash \Lambda_i| \qquad (A6)$$

since $\Lambda_i + R(-\sin \varphi, \cos \varphi) \subset \Lambda$ for every φ. $|\Lambda|$ denotes here the area of the set Λ.

By Eq. (A1) we need the average

$$-\frac{1}{2\pi} \int d\varphi \int d^2x\ \chi_{\Lambda_e}(\mathbf{x}) \chi_\Lambda(x_1 - R \sin \varphi, x_2 + R \cos \varphi)$$

$$\times (x_2 \cos \varphi)$$

$$= \frac{1}{2\pi} \int d\varphi \int d^2x\ \chi_\Lambda(x_1 - R \sin \varphi, x_2 + R \cos \varphi)$$

$$\times (x_2 \cos \varphi) - \frac{1}{2\pi} \int d\varphi \int d^2x\ \chi_{\Lambda_i}(\mathbf{x})$$

$$\times \chi_\Lambda(x_1 - R \sin \varphi, x_2 + R \cos \varphi)(x_2 \cos \varphi). \qquad (A7)$$

The second term is just the interior problem, for which the integral vanishes as in Eq. (A3). The first term equals

$$\frac{1}{2\pi} \int d\varphi \int d^2x\ \chi_\Lambda(\mathbf{x})(R \cos \varphi - x_2) \cos \varphi = |\Lambda| \frac{1}{2} R. \qquad (A8)$$

Thus we conclude that for the normalized average

$$D_{12}^\Lambda = \lim_{\tau \to \infty} \int_0^\infty dt\ e^{-t/\tau} \langle v_2(t) v_1(0) \rangle_\Lambda = \frac{R|\Lambda|}{2|\Lambda \backslash \Lambda_i|}. \qquad (A9)$$

To determine D_{12} we have to compute the double average in Eq. (1.2). With probability one we can choose a large domain Λ (depending on the scatterer configuration) such that if the center of gyration is in Λ, the particle does not collide with a scatterer outside Λ. As before, we shift the configuration in such a way that the center of gyration for $(0, \varphi)$ is still inside Λ. This generates the average $\langle\ \rangle_\Lambda$ and we conclude from Eq. (A9) that this partial average equals $R|\Lambda|/2|\Lambda \backslash \Lambda_i|$. If Λ is large, then for most configurations

$$|\Lambda \backslash \Lambda_i| \cong |\Lambda| e^{-\pi\rho} \qquad (A10)$$

and therefore

$$D_{12} = \frac{1}{2} R e^{\pi\rho}. \qquad (A11)$$

---

[1] A. Lorke, J. P. Kotthaus, and K. Ploog, Phys. Rev. B **44**, 3447 (1991).

[2] K. Ensslin and R. Schuster, in *III-IV Semiconductor Quantum Systems*, edited by K. Ploog (Institution of Electrical Engineers, New York, 1996).

[3] D. Weiss, Phys. Rev. Lett. **66**, 2790 (1991).

[4] T. Schlösser, Ph.D. dissertation, Universität München, 1995 (unpublished).

[5] T. Geisel, A. Zacherl, and G. Radons, Phys. Rev. Lett. **59**, 2503 (1987); Z. Phys. B **71**, 117 (1988).

[6] R. Fleischmann, T. Geisel, and A. Ketzmerick, Phys. Rev. Lett. **68**, 1367 (1992).

[7] M. Fließer, G. J. O. Schmidt, and H. Spohn, Phys. Rev. E **53**, 5690 (1996).

[8] R. Silberbauer, Ph.D. dissertation, Universität Regensburg, 1994 (unpublished).

[9] G. Lütjering, Ph.D. dissertation, Universität Stuttgart, 1996 (unpublished).

[10] H. Spohn, *Large Scale Dynamics of Interacting Particles* (Springer, Berlin, 1991).

[11] M. H. Ernst and A. Weijland, Phys. Rev. A **34**, 39 (1971).

[12] A. Weijland, J. Math. Phys. **15**, 1942 (1974).

[13] W. Götze, E. Leutheußer, and S. Yip, Phys. Rev. A **23**, 2634 (1981); **24**, 100 (1981); **25**, 533 (1982).

[14] E. Leutheußer, Phys. Rev. A **28**, 1762 (1983).

[15] A. J. Masters and T. Keyes, Phys. Rev. A **26**, 2129 (1982); **27**, 2603 (1983).

[16] B. J. Alder and W. E. Alley, J. Stat. Phys. **19**, 341 (1978).

[17] C. P. Lowe and A. J. Masters, Physica A **195**, 149 (1993).

[18] W. Götze and E. Leutheußer, Z. Phys. B **45**, 85 (1981).

[19] A. V. Bobylev, F. A. Maao, A. Hansen, and E. H. Hauge, Phys. Rev. Lett. **75**, 197 (1995).

[20] B. J. Alder and T. E. Wainwright, Phys. Rev. A **1**, 18 (1970).

[21] H. van Beijeren, Rev. Mod. Phys. **54**, 195 (1982).